Small GTPase ARF6 Is a Coincidence-Detection Code for RPH3A Polarization in Neutrophil Polarization

Chunguang Ren,* Qianying Yuan,* Xiaoying Jian,† Paul A. Randazzo,† Wenwen Tang,* and Dianqing Wu*

Cell polarization is a key step for leukocytes adhesion and transmigration during leukocytes' inflammatory infiltration. Polarized localization of plasma membrane (PM) phosphatidylinositol-4-phosphate (PtdIns4P) directs the polarization of RPH3A, which contains a PtdIns4P binding site. Consequently, RPH3A mediates the RAB21 and PIP5K1C90 polarization, which is important for neutrophil adhesion to endothelia during inflammation. However, the mechanism by which RPH3A is recruited only to PM PtdIns4P rather than Golgi PtdIns4P remains unclear. By using ADP-ribosylation factor 6 (ARF6) small interfering RNA, ARF6 dominant-negative mutant ARF6(T27N), and ARF6 activation inhibitor SecinH3, we demonstrate that ARF6 plays an important role in the polarization of RPH3A, RAB21, and PIP5K1C90 in murine neutrophils. PM ARF6 is polarized and colocalized with RPH3A, RAB21, PIP5K1C90, and PM PtdIns4P in mouse and human neutrophils upon integrin stimulation. Additionally, ARF6 binds to RPH3A and enhances the interaction between the PM PtdIns4P and RPH3A. Consistent with functional roles of polarization of RPH3A, Rab21, and PIP5K1C90, ARF6 is also required for neutrophil adhesion on the inflamed endothelial layer. Our study reveals a previously unknown role of ARF6 in neutrophil polarization as being the coincidence-detection code with PM PtdIns4P. Cooperation of ARF6 and PM PtdIns4P direct RPH3A polarization, which is important for neutrophil firm adhesion to endothelia. ***The Journal of Immunology*****, 2020, 204: 1012–1021.**

Leukocytes including neutrophils, monocytes, and lymphocytes, are immune cells that protect the body against both infectious diseases and foreign invaders. Leukocytes respond to inflammation, infection, and injury by leaving the intravascular compartment in a process called leukocyte recruitment. This process involves several distinct steps: selectin-mediated rolling, firm adhesion via integrins, leukocyte crawling, and, finally, transmigration into tissue (1–3). Cell migration is critical for leukocyte inflammatory recruitment (1, 2, 4, 5). Cell polarization is often characterized by asymmetric distribution and organization of cellular signaling and structural molecules. Cell polarization is a key step for cell migration. Meanwhile, cell polarization confers the directionality of cell migration (6–9). Chemoattractants consist of bacterial by-products, complement factors, and chemokines. Through their G protein–coupled receptors, chemoattractants function as dominant inducers for the neutrophil cytoskeleton polarization. This neutrophil cytoskeleton polarization is generally presented by the formation of lamellar F-actin at the leading edge (the front) and actomyosin at the uropod (the back) (10, 11), respectively. Of note, this "back" polarization provides pushing force for cell locomotion; it is also important for neutrophil firm adhesion to the endothelium during neutrophil infiltration (12–15). Importantly, integrin signaling and local plasma membrane (PM) curvature change can cause neutrophil polarization in a manner that is independent of, but instructive to, chemoattractant signaling (14, 16, 17). Integrin signaling confers neutrophils polarity by inducing type I phosphatidylinositol 4-phosphate 5-kinase isoform γ (PIP5K1C90) polarization (14), which further enhances the chemokine-induced RhoA activity in the back of neutrophils. Then, this activated RhoA promotes the formation of actomyosin at the uropod, which is important for neutrophil firm adhesion on the inflammatory endothelium (14). The mechanism, regarding the causative role of integrin in PIP5K1C90 polarization in neutrophils, has been elucidated (16). Integrin stimulation triggers the formation of Rab21 vesicles carrying PIP5K1C90, then Rab21 recruits RPH3A, which targets the vesicle to a polarized destination on neutrophil PM (16). Recently, we identified a PM target for RPH3A in this polarization process, which is PM phosphatidylinositol (PtdIns)–4P. Additionally, we found that local PM curvature increase, resulting from the neutrophil attachment on the inflamed blood vessel before the integrin/chemokine stimulation, induces PM PtdIns4P polarization. This PM PtdIns4P polarization acts upstream of the polarization events, including RPH3A, RAB21, and PIP5K1C90 polarization (17). As the most abundant monophosphorylated

*Department of Pharmacology, Vascular Biology and Therapeutic Program, School of Medicine, Yale University, New Haven, CT 06520; and †Laboratory of Cellular and Molecular Biology, National Cancer Institute, National Institutes of Health, Bethesda, MD 20892

ORCIDs: 0000-0003-3245-1159 (C.R.); 0000-0003-3556-0553 (X.J.).

Received for publication September 3, 2019. Accepted for publication December 10, 2019.

This work was supported by National Institutes of Health Grants R35HL135805 (to D.W.) and R01HL145152 (to W.T.).

D.W. and W.T. supervised the project and developed the concepts. C.R., Q.Y., and X.J. performed experiments and analyzed data. D.W., W.T., C.R., Q.Y., X.J., and P.A.R. designed the experiments and wrote the paper. All authors were involved in the writing and final approval of the manuscript.

Address correspondence and reprint requests to Dr. Wenwen Tang and Dr. Dianqing Wu, Department of Pharmacology, Vascular Biology and Therapeutic Program, Yale University, Room 337e, 10 Amistad Street, New Haven, CT 06520. E-mail addresses: wenwen.tang@yale.edu (W.T.) and dan.wu@yale.edu (D.W.)

The online version of this article contains supplemental material.

Abbreviations used in this article: ARF1, ADP-ribosylation factor 1; ARF6DN, GTP-binding defective mutant of ARF6, T27N; 3D, three-dimensional; Fb, fibrinogen; GEF, guanine nucleotide exchange factor; PIP5K1C90, type I phosphatidylinositol 4-phosphate 5-kinase isoform γ; PK, polylysine; PM, plasma membrane; PtdIns, phosphatidylinositol; siARF6, ARF6 small interfering RNA; siCtr, control small interfering RNA; TGN, *trans*-Golgi network.

inositol phospholipid in mammalian cells, PtdIns4P regulates membrane trafficking, membrane identity, and cell polarity in addition to functioning as the precursor of PtdIns(4,5)P(2) (18–20). PtdIns4P has been detected most abundantly in Golgi and PM (19, 21, 22). So far, the mechanism for the specific docking of PIP5K1C90 vesicles at the PM, rather than Golgi, is still unknown. Generally, the affinities between PtdIns lipids and cytosolic proteins are low. High-affinity interactions of cytosolic proteins with specific membranes are often achieved through the cooperation of PtdIns lipid binding with the binding of other membrane proteins, a process termed as coincidence detection (23). Golgi PtdIns4P and activated ADP-ribosylation factor 1 (ARF1) mediate coincidence detection of four-phosphate-adaptor protein 1 (FAPP1) protein, which directs FAPP1 recruitment to *trans*-Golgi network (TGN) membrane to regulate secretory transport from the TGN (24).

The ARF6 is a small GTPase that locates at the PM, cytosol, and endosomal membranes. ARF6 functions by cycling between an active GTP-bound and inactive GDP-bound conformation. ARF6 regulates diverse cellular processes including exocytosis, endocytosis, endosomal recycling, and actin cytoskeleton remodeling, which underlines its important roles in cell motility, cell polarity, cell division, phagocytosis, and cholesterol homeostasis (25–27). Cytohesin-1, the guanine nucleotide exchange factor (GEF) for ARF6 in leukocytes (28, 29), has been shown to regulate leukocytes adhesion to the chemoattractants stimulated endothelia or ICAM1-coated surface (29–34). This regulation is mediated by molecular interaction of cytohesin-1 with the β2 integrin, as well as by the GEF activity of cytohesin-1. Additionally, ARF6 plays a direct role in the transendothelial chemotaxis of leukocytes triggered by chemokines in both monocytic Mono Mac 6 cells and lymphocytic SK-β2.7 cells (29). ARF6 also activates lipid-modifying enzymes phospholipase D (PLD) and PtdIns 4-phosphate 5-kinase (PIP5-kinase), which promotes the production of PtdIns-4,5-bisphosphate (PIP2) (28, 35–37). Through this, ARF6 regulates multiple neutrophil functions, including superoxide production, degranulation, and chemotaxis (35–37). Of note, the direct role of ARF6 in neutrophil adhesion and polarization during neutrophil recruitment remains unknown. We previously showed that ARF6 is involved in the PIP5K1C90 polarization in neutrophils (14); however, the exact mechanism by which ARF6 regulates PIP5K1C90 polarization has not been investigated.

In this study, we report that ARF6 at the PM functions as a coincidence code for RPH3A protein. ARF6 enhances the interaction of RPH3A with PM PtdIns4P to direct polarization of RPH3A and its downstream events, including RAB21 and PIP5K1C90 polarization, which is important for neutrophil adhesion. Our data have thus revealed an unexpected role of ARF6 in vesicle trafficking and cell polarization in neutrophils.

Materials and Methods

Reagents and constructs

Abs to the following Ags were acquired commercially: ARF6 (PIPA1093×; Thermo Fisher Scientific, for immunofluorescence staining; 5740; Cell Signaling, for Western blot analysis), active ARF6-GTP (26918; NewEast Biosciences, for immunofluorescence staining), TGN38 (sc-27680; Santa Cruz Biotechnology), the 6× histidine tag (2366; Cell Signaling), RAB21 (R4405; Sigma-Aldrich), RPH3A (ARP59498_P050; Aviva Systems Biology), EEA1 (612006; BD Biosciences), β-actin (4970; Cell Signaling), β-tubulin (2146; Cell Signaling), phospho–myosin L chain 2 (3675; Cell Signaling), and PtdIns4P (Z-P004; Echelon Biosciences). The PIP5K1C90 Ab was kindly provided by Dr. P. De Camilli (38). The following reagents were also acquired commercially: fibrinogen (Fb; F3879; Sigma-Aldrich), ICAM-1–Fc (796-IC-050; R&D Systems), SecinH3 (10009570; Cayman Chemical), Alexa Fluor 488 Phalloidin (A12379; Thermo Fisher Scientific), Zombie Violet Fixable Viability dye (423113; BioLegend), and rapamycin (553210; MilliporeSigma). The cDNAs for RAB21, RPH3A, and ARF6 were acquired from Open Biosystems (Lafayette, CO). ARF6 wild-type and mutant T27N were expressed with TagRFP or GFP, and GFP-P4M plasmid was acquired from Addgene. The Lyn11-FRB-mCherry, FKBP-INPP5E, and FKBP-SAC constructs were kindly provided by Dr. T. Balla (39). The control small interfering RNA (siCtr) was from Life Technologies (AM4611), and the ARF6 small interfering RNA (siARF6) is the SMARTpool ON-TARGETplus Arf6 small interfering RNA from Dharmacon (L-043217-01-0005; GE Healthcare).

Mice

Wild-type C57BL mice used for neutrophil isolation were purchased from The Jackson Laboratory. Every housing cage contained no more than five mice. Eight-week-old females were used for primary neutrophils isolation. All animal studies were approved by the institutional animal care and use committees of Yale University.

Cell culture

Mouse endothelial cells (40) were cultured in DMEM supplemented with 10% FBS, 4 mM L-glutamine, and 100 U penicillin and streptomycin. Cells were kept in a 5% CO_2 incubator at 37°C.

Mouse neutrophil preparation and transfection

Murine neutrophils were purified from bone marrows as previously described (41). Briefly, bone marrow cells collected from mice were treated with the ammonium–chloride–potassium buffer (155 mM NH_4Cl, 10 mM $KHCO_3$, and 127 μM EDTA) for RBC lysis, followed by a discontinuous Percoll density gradient centrifugation. Neutrophils were collected from the band located between 81 and 62% of Percoll. The transient transfection of neutrophils was done as previously described (14, 16, 17, 41–47). In brief, three million neutrophils were electroporated with 1.6 μg endotoxin-free plasmids or 300 nM of small interfering RNA using the human monocyte nucleofection kit (Lonza, Zurich, Switzerland) with an Amaxa electroporation system. The cells were then cultured in the medium supplied with the kit containing 10% FBS and 25 ng/ml rGM-CSF (PeproTech, Rocky Hill, NJ) for periods indicated in the figure legends. Cell sorting was done by an FACSAria sorter (BD Biosciences, San Jose, CA). For cell viability analysis, neutrophils were stained with the Zombie Violet Fixable Viability dye, followed by incubation with APC anti-CD11b (17-0112-82; eBioscience) and PerCP-Cy5.5 anti–Ly-6G (560602; BD Biosciences) and analyzed on a BD LSR II flow cytometer.

Human neutrophil preparation

Human neutrophils were isolated as previously described (48). Briefly, peripheral blood was collected from healthy, nonpregnant women and used immediately. Neutrophils were isolated by density centrifugation over a Histopaque 1077/1119 gradient (Sigma-Aldrich). Neutrophils were washed with HBSS without calcium or magnesium (Life Technologies), and hypotonic RBC lysis was performed. The isolated neutrophil fraction was >95% pure, as determined by CD16b staining (1:100 dilution, no. 302005; BioLegend, San Diego, CA) by flow cytometric analysis (FACSCalibur; BD Biosciences). Human tissue collection was approved by the Yale University's Human Research Protection Program (no. 0607001625).

Immunostaining and observation of neutrophils

Neutrophils were fixed with 4% paraformaldehyde for 10 min and permeabilized with 0.01% saponin for 5 min and blocked with 2% BSA in PBS for 1 h. Cells were then incubated with 1:100 diluted primary Abs in blocking buffer at 4°C overnight, followed by incubation of fluorescence conjugated secondary Abs (Alexa 488 colored in green and Alexa 633 colored in red in the figures) with 1:200 dilution for 1 h at room temperature. Slides were prepared with the mounting medium containing DAPI and imaged under a Leica SP5 confocal microscopy.

Quantification of polarization of immunostained proteins in neutrophils was done as previously described (16). Briefly, if the fluorescence intensity in 25% of the cell periphery is accounted for more than 50% of the total fluorescence intensity of the cell periphery, we call the cell polarized.

For colocalization quantification, Z stack images of consecutive optical planes spaced by 0.2 μm were acquired to cover the whole-cell volume using confocal microscopy. Pearson coefficient was determined using Imaris 7.2.3. The three-dimensional (3D) images were reconstructed using Imaris 7.2.3 with a surface rendering model and further adjusted with ImageJ (v1.48K).

Flow chamber assay

To examine neutrophil adherence to endothelial cells under shear stress, mouse endothelial cells (40) were cultured to confluency on 10 ng/ml

Fb-coated coverslips and treated with 50 ng/ml TNF-α (PeproTech) for 4 h at 37°C. The coverslips containing the endothelial cell layer were washed with PBS and placed in a flow chamber apparatus (GlycoTech). The siCtr- and siARF6-transfected neutrophils were labeled with 1 μM CFSE (Thermo Fisher Scientific) and 1 μM Far Red (Thermo Fisher Scientific), respectively, and mixed at 1:1 ratio, then flowed into the chamber at a shear flow rate of 1 dyn/cm^2. The adherent cells were then examined and counted under a widefield fluorescence microscope. We alternated the labeled group in the study to eliminate the possibility of any influence from the dye.

To examine polarization in neutrophils that are adhered to endothelial cells under shear stress, neutrophils were flowed through the chamber seeded with mouse endothelial cells pretreated with TNF-α at a shear flow rate of 1 dyn/cm^2 and imaged by a confocal microscope.

Preparation and purification of recombinant proteins and pull-down assay

Full-length RPH3A and RAB21 were expressed in *Escherichia coli* BL21(DE3) and purified by affinity purification. Myristoylated ARF6 protein and p-RPH3A protein were prepared as described in (49) and (16), respectively. For the pull-down assays, recombinant RAB21 protein or myristoylated ARF6 protein (0.2 mg/ml in 10 μl dissolved in buffer A containing 10 mM phosphate buffer [pH 7.4], 10% glycerol, and 0.2 mM EDTA) was added with 1 μl of 10 mM GDPγS or GTPγS stock (dissolved in 50 mM Tris-HCl [pH 7.8]) for a final concentration of 1 mM guanine nucleotides and incubated on ice for 15 min. Then, RPH3A (0.2 mg/ml in 10 μl dissolved in buffer A) and 180 μl buffer B (10 mM phosphate buffer [pH 7.4], 10% glycerol, 1% Triton X-100, 0.1% SDS, 3 mM DTT, protease inhibitor mixture, 10 mM $MgCl_2$, and 0.1 mM GTPγS or GDPγS, with 0.1 mM $CaCl_2$) were added to RAB21 or ARF6 protein and incubated at 4°C on a rotating platform for overnight. The protein mixture was then added to Ni-NTA Agarose Beads (GE Healthcare) preblocked with 1% BSA and incubated at 4°C on a rotating platform for 2 h. After the beads were washed six times with buffer B, immune complexes were released from the beads by boiling and analyzed by Western blotting.

Buoyant density flotation of liposome assay

The assay was performed as previously described (50) with modifications. Liposomes were consisted of 87% phosphocholine and 9% phosphatidylserine, which were purchased from Avanti Polar Lipids, with 4% PtdIns4P (Echelon Biosciences), and were generated by freezing/thawing five times using liquid nitrogen. Myristoylated ARF6 (2 μg) preloaded with GTPγS or GDPγS was added to the liposome solution and followed by sonication in a bath sonicator for 10 min. Then, the liposome solution was incubated with His-RPH3A proteins (2 μg) for 30 min at room temperature in 150 μl of 25 mM HEPES (pH 7.4), 100 mM KCl, 10% glycerol, and 1 mM DTT (reconstitution buffer). Liposome binding reactions were conducted in the presence of 100 μM of free Ca^{2+}. One hundred and fifty microliters of 80% Accudenz was added to the binding reaction to yield a final concentration of 40% Accudenz. Thirty percent Accudenz and reconstitution buffers were then layered on top and centrifuged for 4 h in a TLA-100 rotor at 32,000 rpm. The liposome layer was collected for Western analysis.

Quantification and statistical analysis

Statistical tests were performed with GraphPad Prism software (version 7.0). All data are presented as the mean ± SEM. Comparisons between the mean variables of two groups were made by two-tailed Student *t* test. Any *p* values of $p < 0.05$ ($^*p < 0.05$, $^*p < 0.01$, $^*p < 0.001$, and $^*p < 0.0001$) were considered to indicate statistical significance. Detailed statistical information about the number of biological replicates, number of cells, and the number of animals were described in the figure legends.

Results

ARF6 is required for RPH3A and RAB21 polarization in neutrophil

To understand how ARF6 regulates the PIP5K1C90 polarization, we investigated the roles of ARF6 in the polarization of RPH3A and RAB21, the two PIP5K1C90 polarization upstream regulators, in an integrin ligand Fb-stimulated mouse neutrophils. siARF6-mediated gene silencing and a dominant-negative, GTP-binding defective mutant of ARF6, T27N (ARF6DN), were employed to study the RPH3A and RAB21 polarization in Fb-stimulated neutrophils. Near 70% ARF6 protein was depleted by siARF6 transfection compared with that of siCtr transfection (Supplemental Fig. 1A). The expression of ARF6DN fused with TagRFP was also validated by Western blot (Supplemental Fig. 1D). We monitored the cell viability of siARF6- or ARF6DN-transfected neutrophils by staining with the cell viability dye and analyzing it by flow cytometry. The result showed that all the transfected neutrophils, which were selected by sorting and used in this study, were

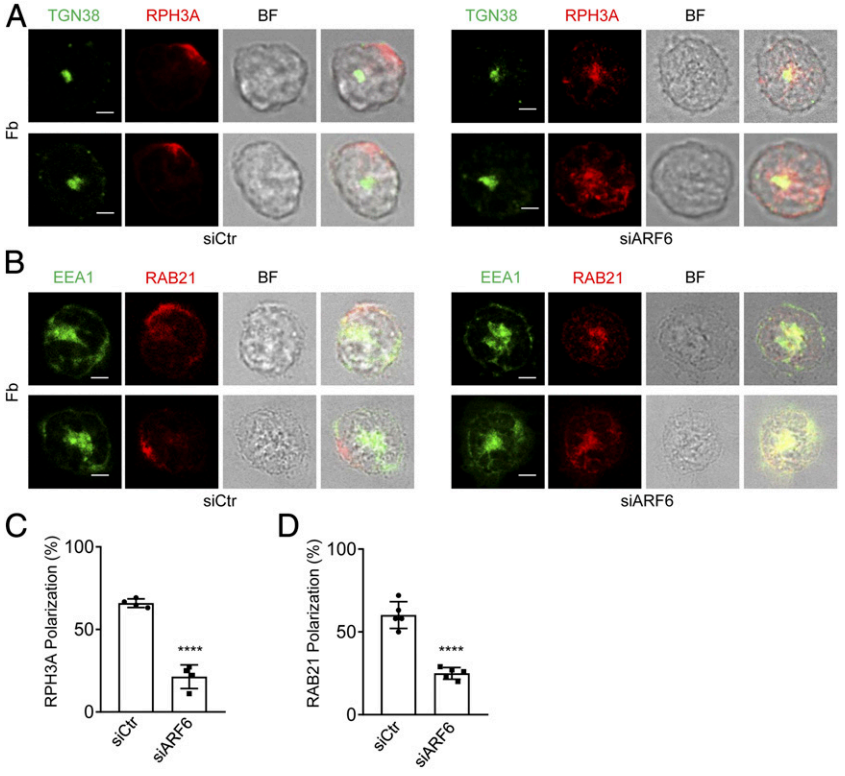

FIGURE 1. RPH3A and RAB21 polarizations are compromised in siARF6-transfected mouse neutrophils. (**A**–**D**) ARF6-knockdown impairs RPH3A and RAB21 polarization. Mouse neutrophils were cotransfected with GFP plasmid and siCtr or siARF6 and cultured for 48 h; GFP-positive cells were sorted out by FACS and attached onto Fb-coated surface before being stained by anti-RPH3A and anti-TGN38 (A) or anti-RAB21 and anti-EEA1 (B), followed with Alexa 633 (red)– and Alexa 488 (green)–conjugated secondary Abs, respectively. Representative optical section images of two cells are shown (A and B). Quantification of polarization was performed as described in the *Materials and Methods* and is shown in (C) and (D). Each data point represents the average of more than 10 cells per observation field, and the experiment was repeated four times. Data are present in means ± SEM (Student *t* test). TGN38 is a resident integral membrane protein of the TGN and thus used as a marker for TGN. Scale bar, 3 μm. $^{****}p < 0.0001$.

viable (Supplemental Fig. 1B, 1C, 1E, 1F). Both siARF6 and ARF6DN expression significantly inhibited polarization of RPH3A and RAB21 in the neutrophils (Figs. 1A–D, 2A–D). SecinH3 is a selective inhibitor for cytohesin-1, which is the GEF for ARF6 in leukocytes (28, 29). To further confirm the effects of ARF6 deficiency on neutrophil polarization, we used SecinH3 to inhibit ARF6 activation in mouse neutrophils. We found the SecinH3 treatment also caused a deficient polarization of RPH3A, RAB21, and PIP5K1C90 in Fb-stimulated neutrophil (Fig. 2E–G). These results together suggest that ARF6 has an important role in the RPH3A–RAB21–PIP5K1C90 polarization pathway.

ARF6 polarizes with RPH3A and PtdIns4P at neutrophil PM

We next examined the localization of active ARF6 by immunofluorescence staining with an ARF6-GTP–specific mouse mAb. We found the polarized localization of active form of ARF6 together with RPH3A, RAB21, and PIP5K1C90 at PM of mouse neutrophils stimulated by Fb (Fig. 3A–C). Interestingly, the ARF6 was not polarized in the neutrophils attaching to a polylysine (PK)–coated surface under a shear stress condition in which the PM PtdIns4P was polarized (Supplemental Fig. 4A) (17). Those results suggest that Fb-mediated integrin activation induces the ARF6 polarization in attached mouse neutrophils. Although Fb can function as a ligand for multiple integrins including αMβ2 (Mac-1), α5β1, αvβ3, and αIIbβ3 (51), our previous study demonstrated that the β2 integrin is the major integrin receptor for Fb to induce PIP5K1C90 polarization in mouse neutrophils (14). During neutrophil inflammatory transendothelial migration, ICAM1 is a major adhesion molecule expressing on the inflamed endothelia to specifically interact with and activate the

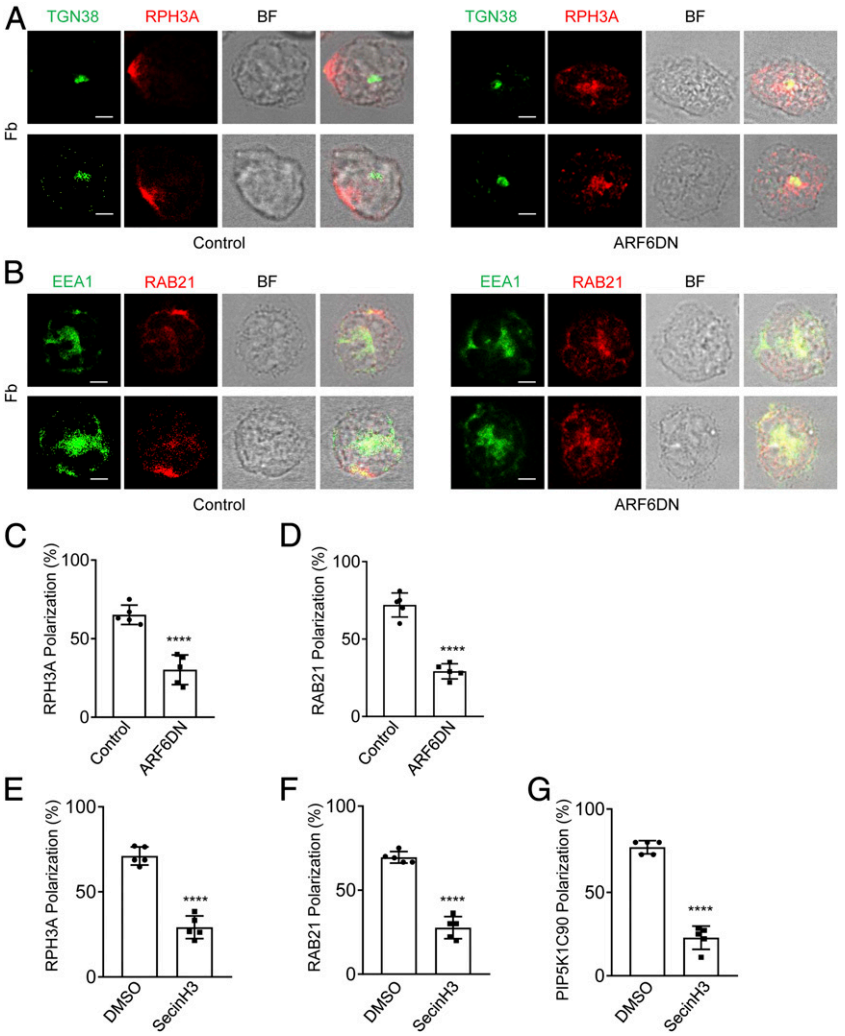

FIGURE 2. ARF6DN and SecinH3 inhibit RPH3A and RAB21 polarization in mouse neutrophils. (**A**–**D**) ARF6 dominant-negative (DN; T27N) mutant impairs RPH3A and RAB21 polarization in mouse neutrophils. Mouse neutrophils were transfected with ARF6DN-TagRFP (ARF6DN) or TagRFP (control). The next day, RFP-positive cells were sorted out by FACS and placed on Fb-coated coverslips for 30 min, followed by immunostaining with anti-RPH3A and anti-TGN38 (A) or anti-RAB21 and anti-EEA1 (B), followed with Alexa 633 (red)– and Alexa 488 (green)–conjugated secondary Abs, respectively. Representative optical section images of two cells are shown. Quantification of polarization of RPH3A and RAB21 was performed as described in the *Materials and Methods* and shown in (C) and (D), respectively. Each data point represents the average of more than 15 cells per observation field, and the experiment was repeated three times. Data are present in means ± SEM (Student *t* test). Scale bar, 3 μm. (**E**–**G**) SecinH3 impairs RPH3A, RAB21, and PIP5K1C90 polarization in mouse neutrophils on the Fb-coated surface. Mouse neutrophils were pretreated with DMSO or 20μM SecinH3 for 20 min at room temperature (RT) and then placed on an Fb-coated coverslip for 30 min along with the DMSO or SecinH3 treatment and subjected to immunostaining with anti-RPH3A and anti-TGN38 (E), anti-RAB21 and anti-EEA1 (F), or anti-PIP5K1C90 and anti-EEA1 (G), followed with Alexa 633 (red)– and Alexa 488 (green)–conjugated secondary Abs, respectively. Quantifications of polarization of RPH3A, RAB21, and PIP5K1C90 are shown in (E)–(G), respectively. Each data point represents the average of more than 15 cells per observation field, and the experiment was repeated four times. Data are present in means ± SEM (Student *t* test). ****$p < 0.0001$. BF, bright field.

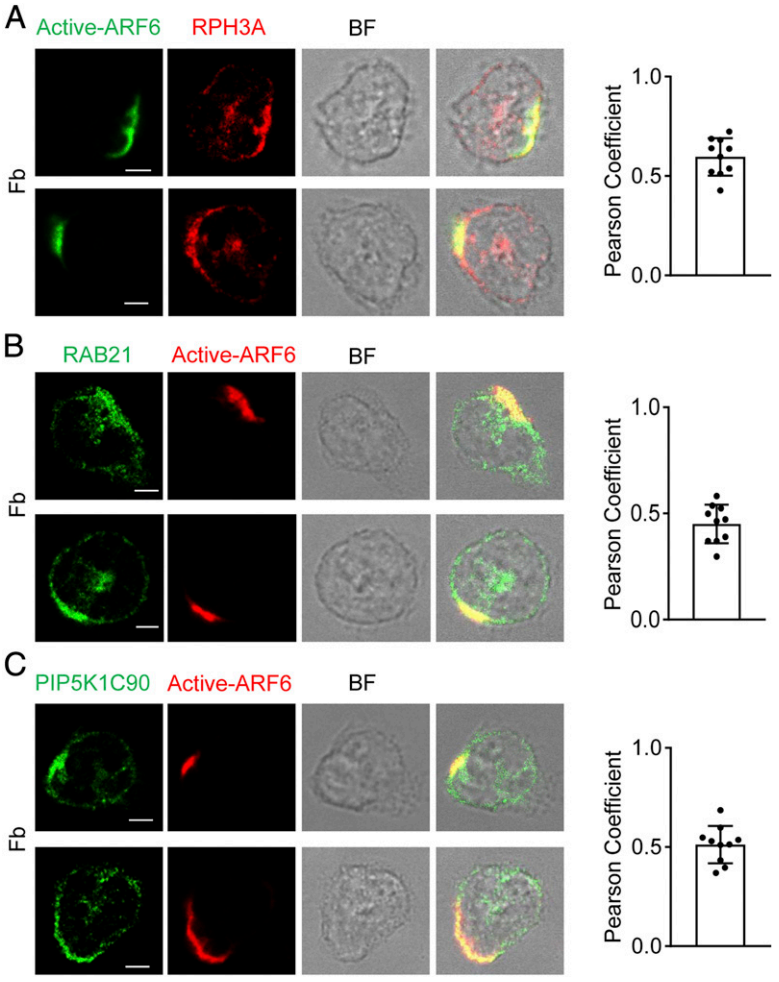

FIGURE 3. ARF6 is copolarized with RPH3A, RAB21, and PIP5K1C90 in Fb-stimulated neutrophils. (**A**–**C**) Copolarization of active ARF6 with RPH3A (A), RAB21 (B), and PIP5K1C90 (C) in neutrophils. Neutrophils attached to Fb-coated surfaces were stained with anti-active ARF6 and anti-RPH3A (A), anti-RAB21 (B), or anti-PIP5K1C90 (C), followed with Alexa 488 (green)– and Alexa 633 (red)–conjugated secondary Abs, respectively. Representative optical section images of two cells are shown. The quantification of colocalization is presented as Pearson correlation coefficient (Pearson Coefficient). Each data point represents a cell. The experiments were repeated three times. Scale bar, 3 μm. BF, bright field.

neutrophil β2 integrins, including αMβ2 (Mac-1) and αLβ2 (LFA-1) (52). To further confirm that β2 integrin is important for ARF6 polarization in neutrophils, we also tested ICAM1. The immunostaining result showed that ARF6 was copolarized with RPH3A, RAB21, and PIP5K1C90 in neutrophils attached to an ICAM1-coated surface (Fig. 4A–C). Besides, SecinH3 inhibited ICAM1-induced polarization of RPH3A, RAB21, and PIP5K1C90 (Fig. 4D–F). Those data suggest that β2 integrin mediates Fb or ICAM1-induced ARF6 polarization. Considering that chemoattractants such as fMLF could activate leukocyte β2 integrin, we tested if fMLF could induce the ARF6 polarization. The ARF6 was found to copolarize with RPH3A, RAB21, and PIP5K1C90 in the fMLF-treated neutrophils attaching to a PK-coated surface, whereas none of those proteins was polarized in neutrophils under the PK-only condition (Supplemental Fig. 2). Finally, we checked the polarization of ARF6, RPH3A, RAB21, and PIP5K1C90 in the human neutrophils under various conditions, including ICAM1, Fb, and PK. Like the mouse neutrophils, the human neutrophils stimulated with Fb or ICAM1 also showed polarized ARF6, which is colocalized with RPH3A, RAB21, and PIP5K1C90, whereas the ARF6 was not polarized in human neutrophils under the PK condition (Supplemental Fig. 3). This finding suggested a conserved role of β2 integrin in inducing the polarization of ARF6, RPH3A, RAB21, and PIP5K1C90 in mouse and human neutrophils. Taken together, those ARF6 localization analyses in neutrophils under various conditions indicate an important role of β2 integrin in ARF6 polarization in neutrophils.

We have recently shown that PM PtdIns4P directs polarization of RAB21, RPH3A, and PIP5K1C90 via its interaction with RPH3A (17). Thus, we investigated the localization relationship between ARF6 and PtdIns4P by using live-cell imaging. ARF6 was found to be colocalized with GFP-P4M, a PtdIns4P-specific live probe (21), at the PM of neutrophils attached to TNF-α–pretreated endothelial cells under shear flow (Fig. 5A, 5C, Supplemental Videos 1, 2). This observation suggested that ARF6 was polarized to the PtdIns4P-rich compartment at the PM of stimulated neutrophils. However, ARF6 was not polarized and minimally colocalized with PM PtdIns4P in neutrophils attached to a PK-coated surface under shear flow (Fig. 5B, 5C, Supplemental Videos 3, 4), a condition that can induce PM PtfIns4P polarization (17). This result is consistent with above-mentioned finding that endogenous ARF6 was not polarized in neutrophils on a PK-coated surface under shear stress (Supplemental Fig. 4A). Collectively, those localization analyses suggested that, like the RPH3A, RAB21, and PIP5K1C90, ARF6 polarization requires stimulation by extracellular stimuli–like integrin. By contrast, PM PtdIns4P polarization in neutrophils is induced by PM membrane curvature changes that occur during cell attachment to a substrate independently of any extracellular stimuli. Of note, this PM curvature–induced PtdIns4P polarization directs polarization of RPH3A, RAB21, and PIP5K1C90 (17). In other words, the polarization of RPH3A, RAB21, and PIP5K1C90 requires both stimulations by extracellular stimuli such as integrins and PM curvature–induced PtdIns4P polarization. To determine whether PM PtdIns4P also regulates ARF6 polarization, we employed a method to specifically deplete PM PtdIns4P as previously reported (17, 39). We found the PM PtdIns4P does not regulate ARF6 polarization in neutrophils (Supplemental Fig. 4B).

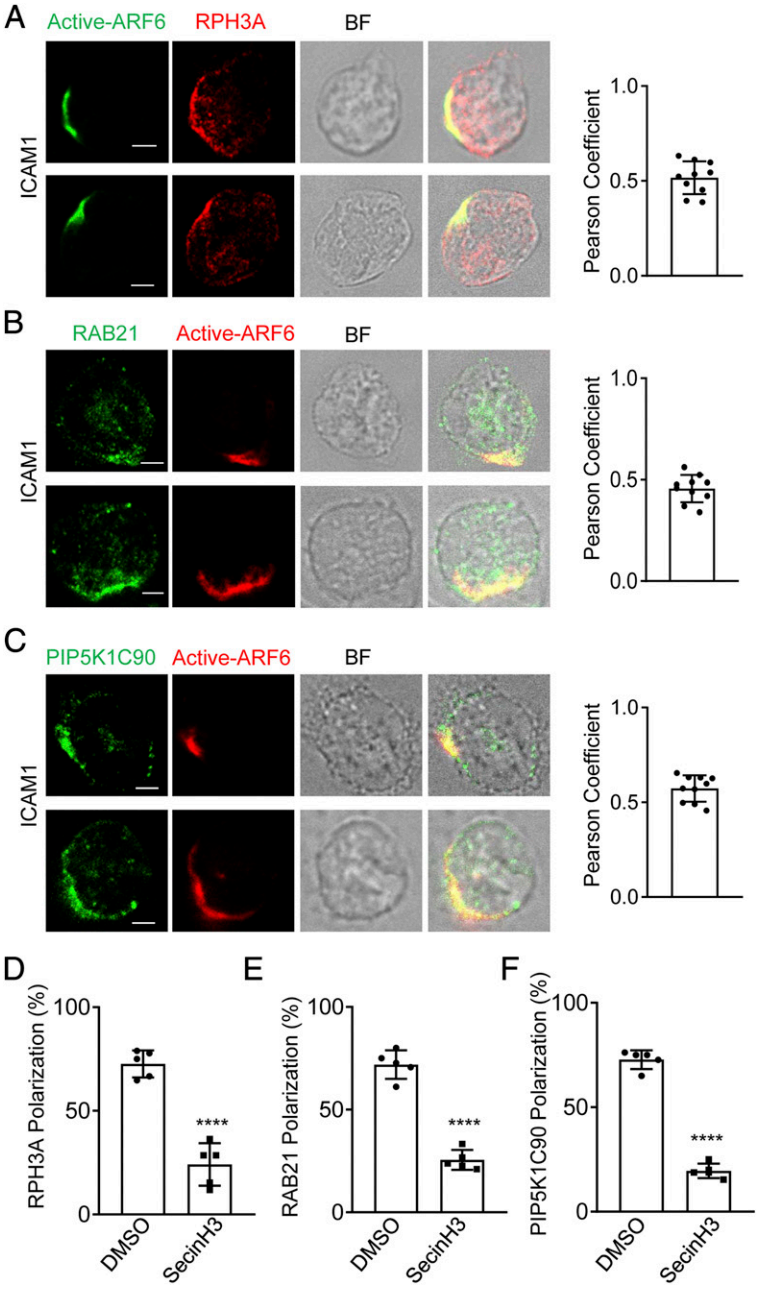

FIGURE 4. ARF6 is copolarized with RPH3A, RAB21, and PIP5K1C90 in ICAM1-stimulated neutrophils. (**A**–**C**) Copolarization of active ARF6 with RPH3A (A), RAB21 (B), and PIP5K1C90 (C) in ICAM1 stimulated mouse neutrophils. Neutrophils attached to ICAM1 (1 μg/ml)–coated surfaces were stained with anti-active ARF6 and anti-RPH3A (A), anti-RAB21 (B), or anti-PIP5K1C90 (C), followed with Alexa 488 (green)– and Alexa 633 (red)–conjugated secondary Abs, respectively. Representative optical section images of two cells are shown. The quantification of colocalization is presented as Pearson correlation coefficient (Pearson Coefficient). Each data point represents a cell. The experiments were repeated four times. Scale bar, 3 μm. BF, bright field. (**D**–**F**) SecinH3 impairs RPH3A, RAB21, and PIP5K1C90 polarization in mouse neutrophils on the ICAM1-coated surface. Mouse neutrophils were pretreated with DMSO or 20 μM SecinH3 for 20 min at RT and then placed on an ICAM1-coated coverslip for 30 min along with the DMSO or SecinH3 treatment and subjected to immunostaining with anti-RPH3A and anti-TGN38 (D), anti-RAB21 and anti-EEA1 (E), or anti-PIP5K1C90 and anti-EEA1 (F), followed with Alexa 633 (red)– and Alexa 488 (green)–conjugated secondary Abs, respectively. Representative optical section images of two cells are shown. Quantification of polarization of RPH3A, RAB21, and PIP5K1C90 is shown in (D)–(F), respectively. Each data point represents the average of more than 15 cells per observation field, and the experiment was repeated three times. Data are present in means ± SEM (Student *t* test). ****$p < 0.0001$.

Thus, ARF6 polarization, in respect of PM PtdIns4P polarization dependency, is different from that of RPH3A, RAB21, and PIP5K1C90.

ARF6 is a coincidence-detection code with PM PtdIns4P for directing RPH3A polarization

Previously, we found that RPH3A direct Rab21 and PIP5K1C90 polarization at the PM by directly interacting with PM PtdIns4P (16, 17). A remaining question was why RPH3A specifically polarizes to PM rather than Golgi, where PtdIns4P is also abundant. As none of RPH3A, RAB21, or PIP5K1C90 is colocalized with the Golgi marker TGN38 (Supplemental Fig. 4C), we postulated that the preferential localization of RPH3A to PM, rather than to Golgi, might be due to RPH3A's coincidence detection of another PM signal in addition to PM PtdIns4P. Small GTPases can function as coincidence-detection codes (24). Immunostaining results indicated that most of the total ARF6 protein, like the active form of ARF6, showed a polarized pattern at the PM without Golgi localization in Fb-stimulated neutrophil (Fig. 5D, Supplemental Fig. 4D). Our above results showed that ARF6 polarization, which occurred at PM, rather than Golgi, acted upstream of RPH3A, RAB21, and PIP5K1C90 polarization but parallel to PtdIns4P polarization. This suggested that ARF6 might function as the coincidence code with PM PtdIns4P for RPH3A polarization at the PM. To test this hypothesis, we assessed the effect of ARF6 on the interaction between PtdIns4P and RPH3A using a coflotation liposome assay in which recombinant myristoylated ARF6 was incorporated into the liposomes containing PtdIns4P. The liposomes containing GTP-bound ARF6 bound a greater amount of RPH3A than those containing GDP-bound ARF6 (Fig. 6A), indicating that active ARF6 enhances the interaction between RPH3A protein and PtdIns4P. Next, we detected the direct interaction between the RPH3A and ARF6 proteins using a pull-down assay with recombinant RPH3A protein and ARF6. The GTP-bound ARF6 showed greater binding of RPH3A than GDP-bound ARF6 (Fig. 6B). We previously demonstrated that RPH3A phosphorylation was

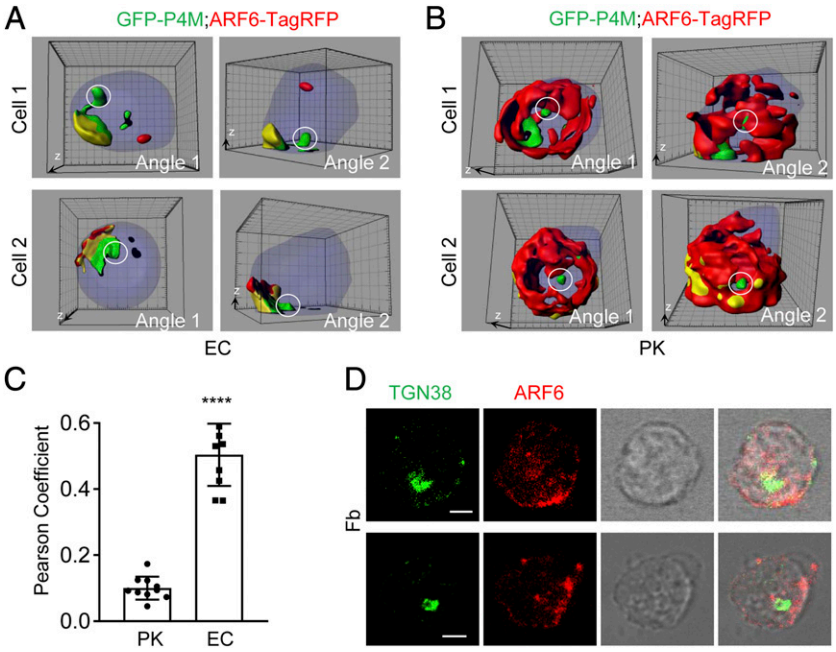

FIGURE 5. ARF6 is copolarized with PM PtdIns4P in neutrophils attaching to activated endothelial cells. (**A**) ARF6 is polarized and colocalized with PM PtdIns4P in mouse neutrophils attached to endothelial cells under shear flow. Mouse neutrophils were transfected with GFP-P4M and ARF6-TagRFP plasmids and cultured for 6 h, then flowed through a chamber seeded with mouse endothelial cells pretreated with TNF-α and observed with a confocal microscope. Reconstructed 3D images of two representative cells are shown. The Golgi pool of PtdIns4P is denoted with a white circle. The 3D whole-cell contour is colored in purple, and the colocalization between PtdIns4P and ARF6 is marked in yellow. Each cell is shown in two different angles, in which angles 1 and 2 are referred to as dorsal view and side view, respectively. The raw 3D images are shown as Supplemental Videos 1, 2. The grid scales are 1 μm. (**B**) ARF6 is not polarized and minimally colocalized with PM PtdIns4P in mouse neutrophils attached to PK-coated surface under shear flow. Mouse neutrophils were transfected with GFP-P4M and ARF6-TagRFP plasmids and cultured for 6 h, then flowed through a chamber coated with polylysine at the rate of 1 dyn/cm^2 and observed with a confocal microscope. Reconstructed 3D images of two representative cells are shown. The Golgi pool of PtdIns4P is denoted with a white circle. The raw 3D images are shown as Supplemental Videos 3, 4. The grid scales are 1 μm. (**C**) Quantification of colocalization of P4M and ARF6 in (A) and (B) conditions is shown as the Pearson coefficient. Each data point represents a cell. Data are presented as means ± SEM (Student *t* test). The experiments were repeated three times. ****$p < 0.0001$. EC, endothelial cell. (**D**) ARF6 is polarized, but not colocalized, with TGN38 in neutrophils on Fb. Mouse neutrophils were placed on Fb for 30 min, followed by immunostaining with the anti-TGN38 and anti-ARF6, then incubated with Alexa 488 (green)– and Alexa 633 (red)–conjugated secondary Abs, respectively. Representative optical section images of two cells are shown. Scale bar, 3 μm.

important for RPH3A and RAB21 interaction and RAB21 and PIP5K1C90 polarization (16). Consistently, in this study, we found that ARF6 preferred binding to p-RPH3A protein, in comparison with unphosphorylated one (Fig. 6C). Finally, we assessed the effect of ARF6 on the interaction between RAB21 and RPH3A using GTP-ARF6, GTP-RAB21, and RPH3A recombinant proteins in a pull-down assay. We found that ARF6 enhanced RAB21–RPH3A interaction (Fig. 6D). Besides, RAB21 did not interfere with the ARF6–RPH3A interaction (Fig. 6D), suggesting that ARF6 and RAB21 have nonoverlapping interaction sites on the RPH3A protein. These results together showed that ARF6 manifested the biochemical characteristic of a coincidence-detection code for RPH3A.

ARF6 regulates neutrophil adhesion

The results above suggest that ARF6 is the coincident detection code for RPH3A protein anchoring at the PM, by which ARF6 mediates the polarized transport of RAB21–RPH3A–PIP5K1C90 vesicles. We previously revealed an important role of polarized PIP5K1C90 and RPH3A in neutrophil firm adhesion to the inflammatory endothelium (14, 16). Consistently, we found siARF6 significantly inhibited neutrophil adhesion to endothelial cells in a flow chamber assay (Fig. 7A–D).

Discussion

In this study, we elucidated the mechanism by which RPH3A specifically targets the PtdIns4P at the PM in neutrophil polarization. Our results demonstrate that ARF6 is a coincidence-detection code for RPH3A, and it works together with PM PtdIns4P to direct the RPH3A–RAB21–PIP5K1C90 polarization pathway, as depicted in a model (Fig. 7E). Namely, Fb, ICAM1, or chemoattractant-activated β2 integrin stimulates the ARF6 polarization at the PM in mouse neutrophils. ARF6 is copolarized with PM PtdIns4P, whose polarization is induced by the PM curvature increase resulting from cell attachment (17). ARF6 and PtdIns4P together present a high-affinity binding site for RPH3A, which may explain the preferential recruitment of RPH3A to PM rather than Golgi. PM polarization of RPH3A results in subsequent PM polarization of RAB21 and PIP5K1C90. Thus, our study has revealed important functions of ARF6 in neutrophil biology, including neutrophils polarization and adhesion on the inflamed blood vessels.

ARF6 was shown to be a direct activator of PIP5K (53). Following that finding, ARF6 was demonstrated to regulate various cellular functions, including endocytosis, endosomal recycling, and actin polymerization, mainly through the activation of PIP5K for PIP2 production (25, 54). In this study, we elucidated a new role of ARF6 in PIP5K1C90 regulation, namely its polarization, in neutrophils. Those observations underline a dual regulatory mechanism ARF6 on PIP5K1C90, both of which may cooperate to regulate neutrophil adhesion. Cytohesin-1, the GEF for ARF6 in leukocytes, controls the activation of RhoA in dendritic cells and HeLa cells (29). This regulation is required for integrin-mediated cell adhesion and migration in a GEF activity–dependent manner

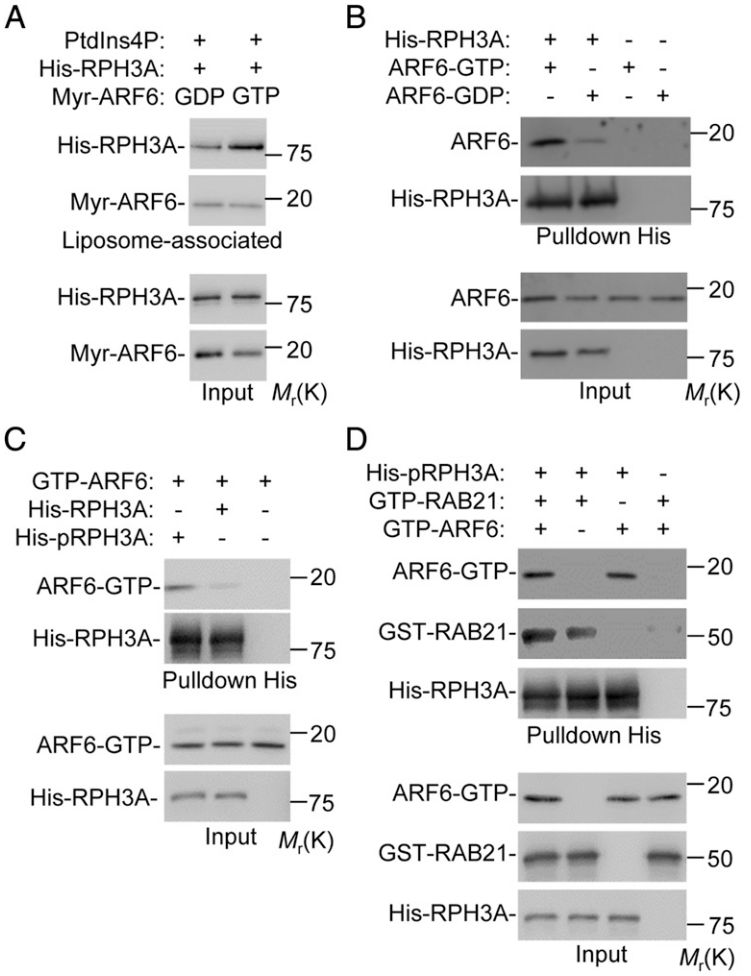

FIGURE 6. ARF6 is a coincidence-detection code for RPH3A protein. (**A**) GTP-bound ARF6 augments the interaction of RPH3A with PtdIns4P. Purified recombinant myristoylated ARF6 protein preloaded with GDPγS or GTPγS was incorporated into phosphocholine (PC)/phosphatidylserine (PS) liposome containing PtdIns4P. The liposomes were then incubated with purified recombinant RPH3A protein, followed by density ultracentrifugation. Input and liposome-associated proteins were detected by Western analysis. (**B**) RPH3A preferentially binds to GTP-bound ARF6. Purified recombinant myristoylated ARF6 protein preloaded with GTPγS or GDPγS was incubated with purified His-tagged recombinant RPH3A protein, followed by nickel-bead pull-down and Western analysis. (**C**) ARF6 preferentially binds to p-RPH3A. Purified recombinant proteins were used in an His–pull-down assay under the conditions described in the figure. Proteins were then detected by Western blot analysis. (**D**) ARF6 augments the interaction between the RPH3A and RAB21. Purified GTPγS-bound myristoylated ARF6 and RAB21 were incubated with p-RPH3A and subjected to an His–pull-down assay. The proteins were detected by Western blot analysis.

(29). However, the mechanistic link between cytohesin-1 and RhoA is unknown. PIP5K1C90 polarization has been shown to regulate chemokine- or integrin-induced neutrophil adhesion by promoting polarized RhoA activation at uropods by chemoattractants and subsequent formation of polarized phosphorylated myosin L chain at uropods (14). Our data suggest that ARF6 regulates PIP5K1C90 polarization in neutrophils, which provide a possible mechanism by which the cytohesin-1 regulates RhoA activity.

cytohesin-1 has been proved to regulate leukocyte adhesion on ICAM1 surfaces or endothelial cells, at least partially, requiring its GEF activity (30–32), suggesting a functional role of its downstream effector GTPases, including ARF6 in leukocyte adhesion. So far, the direct evidence of functional involvement of ARF6 in leukocyte adhesion during leukocyte diapedesis is missing, even though ARF6 can directly regulate superoxide production, degranulation, and chemotaxis in neutrophils (28, 35–37). ARF6 is important for innate immunity and host–pathogen interactions (27), in which ARF6 is involved in TLR signaling, phagocytosis, pathogen invasion, reactive oxygen species production, and MHC class I recycling. To our knowledge, our study, for the first time, demonstrates that ARF6 has a direct role in regulating neutrophil polarization and adhesion through regulating integrin or chemoattractant-induced PIP5K1C90 polarization, which is important for leukocyte adhesion on inflamed endothelia (14, 55). This study may provide a likely mechanism for the important role of cytohesin-1 in leukocyte adhesion as well as the ARF6's involvement in leukocyte transendothelial chemotaxis described in previous studies (29–34). This ARF6 polarization may also contribute to phagocytosis through determining the PIP5K1C90 localization at the PM, as PIP5K-γ is essential for Fcγ receptor–mediated phagocytosis (56).

Although ARF6 has multiple subcellular pools, including PM, endosome, and cytosol (24), in our study, we could not detect obvious localization in the cytosol or endosome. This may be due to the resolution limitation of the confocal imaging or highly preferential PM accumulation of ARF6, which could be transported from the cytosol or endosome pools under Fb stimulation.

Several remaining questions warrant further investigations. We showed that ARF6 polarization required integrin signaling achieved by direct Fb or ICAM1 stimulation or indirect chemoattractant treatment. Besides, integrins, particularly β2 integrin, are involved in polarized localization of PIP5K1C90 in mouse neutrophils (14). β2 integrin is likely the responsive receptor for Fb or ICAM1 for inducing the ARF6 polarization. Interestingly, we found the ARF6 was not polarized on the PK-coated surface even under a shear flow condition, in which the PM PtdIns4P would be polarized (17). This observation is consistent with the previous finding that cytohesin-1 was not polarized on the PK-coated surface (34). However, the molecular mechanism by which integrin signaling regulates ARF6 polarization remains unknown. Besides, ARF6 controls integrin trafficking at multiple steps, including integrin internalization, early endosome trafficking, and recycling back to the PM along microtubules (57, 58). RAB21 regulates β1 integrin endocytosis from the PM to the early endosomes and integrin-mediated cell adhesion and motility (59, 60). Those studies suggest ARF6 cooperates with RAB21 to regulate integrin trafficking. In our previous study,

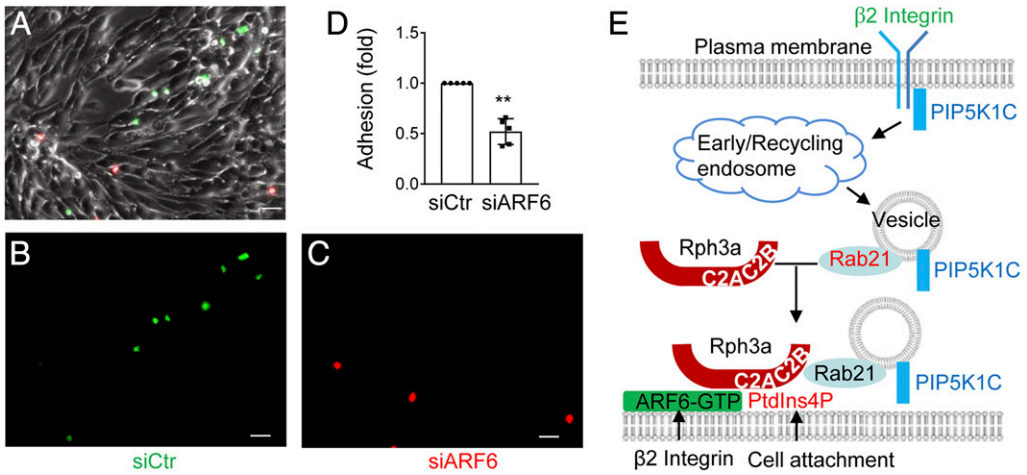

FIGURE 7. ARF6 regulates neutrophil adhesion. (**A**–**D**) ARF6 is important for neutrophil adhesion on the inflamed endothelial layer. Mouse neutrophils were transfected with siCtr or siARF6 for 48 h and were labeled with CFSE and Far Red dyes, respectively, then mixed at 1:1 ratio before flowing through a chamber seeded with endothelial cells pretreated with TNF-α. The adherent neutrophils were imaged under a widefield microscope. Representative images of bright field (A), CFSE (B), and Far Red (C) are shown. The adhesion quantification of the siCtr- or siARF6-transfected neutrophils is also shown (D). Each data point represents one chamber, and the experiment was repeated five times. Data are present in means ± SEM (Student *t* test). Scale bar, 50 μm. $^{**}p < 0.01$. (**E**) Schematic presentation of a model for ARF6 to direct polarized docking of RPH3A–PIP5K1C90 vesicles at the PM. Integrin engagement triggers endocytosis of PIP5K1C90, which traffics through EEA1-positive endosomes and RAB21-positive recycling vesicles, and the GTP-bound RAB21 exits from the endosomes and recruits RPH3A (16), which, in turn, targets the vesicles to PM PtdIns4P with the help of the coincidence-detection code of ARF6, where the PM PtdIns4P polarization is induced by cell attachment (17). This process eventually results in PIP5K1C90 polarization and confers neutrophil adhesion on inflamed endothelium.

we showed the integrin stimulation could induce the polarization of RAB21 (16). In this study, we showed that the integrin induced the polarization of ARF6, and ARF6 polarization further regulated RAB21 polarization. Therefore, there may be complex reciprocal regulation mechanisms among the integrins ARF6 and RAB21. Our results also showed that ARF6 directly binds to RPH3A protein without interfering with the interactions between the RPH3A and RAB21 or PtdIns4P, which suggested their binding sites in the RPH3A protein are nonoverlapping. Further studies are needed to characterize ARF6–RPH3A interaction.

Acknowledgments

We thank Michelle Orsulak (Department of Pharmacology, Yale School of Medicine) for technical assistance in the mice caring and reagents preparation, Mancy Tong (Department of Obstetrics, Gynecology and Reproductive Sciences, Yale School of Medicine) for assistance in human neutrophil preparation, and Pietro De Camilli (Department of Cell Biology, Yale School of Medicine) for providing the PIP5K1C90 Ab.

Disclosures

The authors have no financial conflicts of interest.

References

1. Ley, K., C. Laudanna, M. I. Cybulsky, and S. Nourshargh. 2007. Getting to the site of inflammation: the leukocyte adhesion cascade updated. *Nat. Rev. Immunol.* 7: 678–689.
2. Kolaczkowska, E., and P. Kubes. 2013. Neutrophil recruitment and function in health and inflammation. *Nat. Rev. Immunol.* 13: 159–175.
3. Shi, C., and E. G. Pamer. 2011. Monocyte recruitment during infection and inflammation. *Nat. Rev. Immunol.* 11: 762–774.
4. de Oliveira, S., E. E. Rosowski, and A. Huttenlocher. 2016. Neutrophil migration in infection and wound repair: going forward in reverse. *Nat. Rev. Immunol.* 16: 378–391.
5. Nourshargh, S., and R. Alon. 2014. Leukocyte migration into inflamed tissues. *Immunity* 41: 694–707.
6. Woodham, E. F., and L. M. Machesky. 2014. Polarised cell migration: intrinsic and extrinsic drivers. *Curr. Opin. Cell Biol.* 30: 25–32.
7. Graziano, B. R., and O. D. Weiner. 2014. Self-organization of protrusions and polarity during eukaryotic chemotaxis. *Curr. Opin. Cell Biol.* 30: 60–67.
8. Wang, F. 2009. The signaling mechanisms underlying cell polarity and chemotaxis. *Cold Spring Harb. Perspect. Biol.* 1: a002980.
9. Gómez-Moutón, C., and S. Mañes. 2007. Establishment and maintenance of cell polarity during leukocyte chemotaxis. *Cell Adh. Migr.* 1: 69–76.
10. Petri, B., and M. J. Sanz. 2018. Neutrophil chemotaxis. *Cell Tissue Res.* 371: 425–436.
11. Weiner, O. D., P. O. Neilsen, G. D. Prestwich, M. W. Kirschner, L. C. Cantley, and H. R. Bourne. 2002. A PtdInsP(3)- and Rho GTPase-mediated positive feedback loop regulates neutrophil polarity. *Nat. Cell Biol.* 4: 509–513.
12. Hind, L. E., W. J. Vincent, and A. Huttenlocher. 2016. Leading from the back: the role of the uropod in neutrophil polarization and migration. *Dev. Cell* 38: 161–169.
13. Cramer, L. P. 2010. Forming the cell rear first: breaking cell symmetry to trigger directed cell migration. *Nat. Cell Biol.* 12: 628–632.
14. Xu, W., P. Wang, B. Petri, Y. Zhang, W. Tang, L. Sun, H. Kress, T. Mann, Y. Shi, P. Kubes, and D. Wu. 2010. Integrin-induced PIP5K1C kinase polarization regulates neutrophil polarization, directionality, and in vivo infiltration. *Immunity* 33: 340–350.
15. Sánchez-Madrid, F., and J. M. Serrador. 2009. Bringing up the rear: defining the roles of the uropod. *Nat. Rev. Mol. Cell Biol.* 10: 353–359.
16. Yuan, Q., C. Ren, W. Xu, B. Petri, J. Zhang, Y. Zhang, P. Kubes, D. Wu, and W. Tang. 2017. PKN1 directs polarized RAB21 vesicle trafficking via RPH3A and is important for neutrophil adhesion and ischemia-reperfusion injury. *Cell Rep.* 19: 2586–2597.
17. Ren, C., Q. Yuan, M. Braun, X. Zhang, B. Petri, J. Zhang, D. Kim, J. Guez-Haddad, W. Xue, W. Pan, et al. 2019. Leukocyte cytoskeleton polarization is initiated by plasma membrane curvature from cell attachment. *Dev. Cell* 49: 206–219.e7.
18. Hammond, G. R., and Y. Hong. 2018. Phosphoinositides and membrane targeting in cell polarity. *Cold Spring Harb. Perspect. Biol.* 10: a027938.
19. De Matteis, M. A., C. Wilson, and G. D'Angelo. 2013. Phosphatidylinositol-4-phosphate: the Golgi and beyond. *BioEssays* 35: 612–622.
20. D'Angelo, G., M. Vicinanza, A. Di Campli, and M. A. De Matteis. 2008. The multiple roles of PtdIns(4)P -- not just the precursor of PtdIns(4,5)P2. *J. Cell Sci.* 121: 1955–1963.
21. Hammond, G. R., M. P. Machner, and T. Balla. 2014. A novel probe for phosphatidylinositol 4-phosphate reveals multiple pools beyond the Golgi. *J. Cell Biol.* 205: 113–126.
22. Nakatsu, F., J. M. Baskin, J. Chung, L. B. Tanner, G. Shui, S. Y. Lee, M. Pirruccello, M. Hao, N. T. Ingolia, M. R. Wenk, and P. De Camilli. 2012. PtdIns4P synthesis by PI4KIIIα at the plasma membrane and its impact on plasma membrane identity. *J. Cell Biol.* 199: 1003–1016.
23. Di Paolo, G., and P. De Camilli. 2006. Phosphoinositides in cell regulation and membrane dynamics. *Nature* 443: 651–657.
24. Liu, Y., R. A. Kahn, and J. H. Prestegard. 2014. Interaction of Fapp1 with Arf1 and PI4P at a membrane surface: an example of coincidence detection. *Structure* 22: 421–430.
25. Donaldson, J. G. 2003. Multiple roles for Arf6: sorting, structuring, and signaling at the plasma membrane. *J. Biol. Chem.* 278: 41573–41576.
26. Schweitzer, J. K., A. E. Sedgwick, and C. D'Souza-Schorey. 2011. ARF6-mediated endocytic recycling impacts cell movement, cell division and lipid homeostasis. *Semin. Cell Dev. Biol.* 22: 39–47.

27. Van Acker, T., J. Tavernier, and F. Peelman. 2019. The small GTPase Arf6: an overview of its mechanisms of action and of its role in host¯pathogen interactions and innate immunity. *Int. J. Mol. Sci.* 20: E2209.
28. El Azreq, M. A., V. Garceau, D. Harbour, C. Pivot-Pajot, and S. G. Bourgoin. 2010. Cytohesin-1 regulates the Arf6-phospholipase D signaling axis in human neutrophils: impact on superoxide anion production and secretion. *J. Immunol.* 184: 637–649.
29. Weber, K. S., C. Weber, G. Ostermann, H. Dierks, W. Nagel, and W. Kolanus. 2001. Cytohesin-1 is a dynamic regulator of distinct LFA-1 functions in leukocyte arrest and transmigration triggered by chemokines. *Curr. Biol.* 11: 1969–1974.
30. El azreq, M. A., and S. G. Bourgoin. 2011. Cytohesin-1 regulates human blood neutrophil adhesion to endothelial cells through β2 integrin activation. *Mol. Immunol.* 48: 1408–1416.
31. Quast, T., B. Tappertzhofen, C. Schild, J. Grell, N. Czeloth, R. Förster, R. Alon, L. Fraemohs, K. Dreck, C. Weber, et al. 2009. Cytohesin-1 controls the activation of RhoA and modulates integrin-dependent adhesion and migration of dendritic cells. *Blood* 113: 5801–5810.
32. Geiger, C., W. Nagel, T. Boehm, Y. van Kooyk, C. G. Figdor, E. Kremmer, N. Hogg, L. Zeitlmann, H. Dierks, K. S. Weber, and W. Kolanus. 2000. Cytohesin-1 regulates beta-2 integrin-mediated adhesion through both ARF-GEF function and interaction with LFA-1. *EMBO J.* 19: 2525–2536.
33. Kolanus, W., W. Nagel, B. Schiller, L. Zeitlmann, S. Godar, H. Stockinger, and B. Seed. 1996. Alpha L beta 2 integrin/LFA-1 binding to ICAM-1 induced by cytohesin-1, a cytoplasmic regulatory molecule. *Cell* 86: 233–242.
34. Nagel, W., P. Schilcher, L. Zeitlmann, and W. Kolanus. 1998. The PH domain and the polybasic c domain of cytohesin-1 cooperate specifically in plasma membrane association and cellular function. *Mol. Biol. Cell* 9: 1981–1994.
35. Gamara, J., F. Chouinard, L. Davis, F. Aoudjit, and S. G. Bourgoin. 2015. Regulators and effectors of Arf GTPases in neutrophils. *J. Immunol. Res.* 2015: 235170.
36. Skippen, A., D. H. Jones, C. P. Morgan, M. Li, and S. Cockcroft. 2002. Mechanism of ADP ribosylation factor-stimulated phosphatidylinositol 4,5-bisphosphate synthesis in HL60 cells. *J. Biol. Chem.* 277: 5823–5831.
37. Dana, R. R., C. Eigsti, K. L. Holmes, and T. L. Leto. 2000. A regulatory role for ADP-ribosylation factor 6 (ARF6) in activation of the phagocyte NADPH oxidase. *J. Biol. Chem.* 275: 32566–32571.
38. Di Paolo, G., L. Pellegrini, K. Letinic, G. Cestra, R. Zoncu, S. Voronov, S. Chang, J. Guo, M. R. Wenk, and P. De Camilli. 2002. Recruitment and regulation of phosphatidylinositol phosphate kinase type 1 gamma by the FERM domain of talin. *Nature* 420: 85–89.
39. Hammond, G. R., M. J. Fischer, K. E. Anderson, J. Holdich, A. Koteci, T. Balla, and R. F. Irvine. 2012. PI4P and PI(4,5)P2 are essential but independent lipid determinants of membrane identity. *Science* 337: 727–730.
40. Wang, Z., B. Liu, P. Wang, X. Dong, C. Fernandez-Hernando, Z. Li, T. Hla, Z. Li, K. Claffey, J. D. Smith, and D. Wu. 2008. Phospholipase C beta3 deficiency leads to macrophage hypersensitivity to apoptotic induction and reduction of atherosclerosis in mice. *J. Clin. Invest.* 118: 195–204.
41. Zhang, Y., W. Tang, M. C. Jones, W. Xu, S. Halene, and D. Wu. 2010. Different roles of G protein subunits beta1 and beta2 in neutrophil function revealed by gene expression silencing in primary mouse neutrophils. *J. Biol. Chem.* 285: 24805–24814.
42. Tang, W., Y. Zhang, W. Xu, T. K. Harden, J. Sondek, L. Sun, L. Li, and D. Wu. 2011. A PLCβ/PI3Kγ-GSK3 signaling pathway regulates cofilin phosphatase slingshot2 and neutrophil polarization and chemotaxis. *Dev. Cell* 21: 1038–1050.
43. Zhang, Y., W. Tang, H. Zhang, X. Niu, Y. Xu, J. Zhang, K. Gao, W. Pan, T. J. Boggon, D. Toomre, et al. 2013. A network of interactions enables CCM3 and STK24 to coordinate UNC13D-driven vesicle exocytosis in neutrophils. *Dev. Cell* 27: 215–226.
44. Simunovic, M., G. A. Voth, A. Callan-Jones, and P. Bassereau. 2015. When physics takes over: BAR proteins and membrane curvature. *Trends Cell Biol.* 25: 780–792.
45. Basit, A., W. Tang, and D. Wu. 2016. shRNA-induced gene knockdown in vivo to investigate neutrophil function. *Methods Mol. Biol.* 1407: 169–177.
46. Loison, F., H. Zhu, K. Karatepe, A. Kasorn, P. Liu, K. Ye, J. Zhou, S. Cao, H. Gong, D. E. Jenne, et al. 2014. Proteinase 3-dependent caspase-3 cleavage modulates neutrophil death and inflammation. *J. Clin. Invest.* 124: 4445–4458.
47. Sun, C. X., M. A. Magalhães, and M. Glogauer. 2007. Rac1 and Rac2 differentially regulate actin free barbed end formation downstream of the fMLP receptor. *J. Cell Biol.* 179: 239–245.
48. Tong, M., J. A. Potter, G. Mor, and V. M. Abrahams. 2019. Lipopolysaccharide-stimulated human fetal membranes induce neutrophil activation and release of vital neutrophil extracellular traps. *J. Immunol.* 203: 500–510.
49. Ha, V. L., G. M. Thomas, S. Stauffer, and P. A. Randazzo. 2005. Preparation of myristoylated Arf1 and Arf6. *Methods Enzymol.* 404: 164–174.
50. Boswell, K. L., D. J. James, J. M. Esquibel, S. Bruinsma, R. Shirakawa, H. Horiuchi, and T. F. Martin. 2012. Munc13-4 reconstitutes calcium-dependent SNARE-mediated membrane fusion. *J. Cell Biol.* 197: 301–312.
51. Davalos, D., and K. Akassoglou. 2012. Fibrinogen as a key regulator of inflammation in disease. *Semin. Immunopathol.* 34: 43–62.
52. Li, N., D. Mao, S. Lü, C. Tong, Y. Zhang, and M. Long. 2013. Distinct binding affinities of Mac-1 and LFA-1 in neutrophil activation. *J. Immunol.* 190: 4371–4381.
53. Honda, A., M. Nogami, T. Yokozeki, M. Yamazaki, H. Nakamura, H. Watanabe, K. Kawamoto, K. Nakayama, A. J. Morris, M. A. Frohman, and Y. Kanaho. 1999. Phosphatidylinositol 4-phosphate 5-kinase alpha is a downstream effector of the small G protein ARF6 in membrane ruffle formation. *Cell* 99: 521–532.
54. Funakoshi, Y., H. Hasegawa, and Y. Kanaho. 2011. Regulation of PIP5K activity by Arf6 and its physiological significance. *J. Cell. Physiol.* 226: 888–895.
55. Porciello, N., M. Kunkl, A. Viola, and L. Tuosto. 2016. Phosphatidylinositol 4-phosphate 5-kinases in the regulation of T cell activation. *Front. Immunol.* 7: 186.
56. Mao, Y. S., M. Yamaga, X. Zhu, Y. Wei, H. Q. Sun, J. Wang, M. Yun, Y. Wang, G. Di Paolo, M. Bennett, et al. 2009. Essential and unique roles of PIP5K-gamma and -alpha in Fcgamma receptor-mediated phagocytosis. *J. Cell Biol.* 184: 281–296.
57. De Franceschi, N., H. Hamidi, J. Alanko, P. Sahgal, and J. Ivaska. 2015. Integrin traffic - the update. *J. Cell Sci.* 128: 839–852.
58. Chen, P. W., R. Luo, X. Jian, and P. A. Randazzo. 2014. The Arf6 GTPase-activating proteins ARAP2 and ACAP1 define distinct endosomal compartments that regulate integrin α5β1 traffic. *J. Biol. Chem.* 289: 30237–30248.
59. Pellinen, T., A. Arjonen, K. Vuoriluoto, K. Kallio, J. A. Fransen, and J. Ivaska. 2006. Small GTPase Rab21 regulates cell adhesion and controls endosomal traffic of beta1-integrins. *J. Cell Biol.* 173: 767–780.
60. Mai, A., S. Veltel, T. Pellinen, A. Padzik, E. Coffey, V. Marjomäki, and J. Ivaska. 2011. Competitive binding of Rab21 and p120RasGAP to integrins regulates receptor traffic and migration. *J. Cell Biol.* 194: 291–306.